

# Low Parameter Sensitivity Deadbeat Direct Torque Control for Surface Mounted Permanent Magnet Synchronous Motors

Xiao-Guang Zhang<sup>†,\*</sup>, Ke-Qin Wang<sup>\*</sup>, and Ben-Shuai Hou<sup>\*</sup>

<sup>†</sup>Inverter Technologies Engineering Research Center of Beijing, North China University of Technology, Beijing, China

<sup>\*</sup>Collaborative Innovation Center of Key Power Energy-Saving Technologies in Beijing, North China University of Technology, Beijing, China

## Abstract

In order to decrease the parameter sensitivity of deadbeat direct torque control (DB-DTC), an improved deadbeat direct torque control method for surface mounted permanent-magnet synchronous motor (SPMSM) drives is proposed. First, the track errors of the stator flux and torque that are caused by model parameter mismatch are analyzed. Then a sliding mode observer is designed, which is able to predict the d-q axis currents of the next control period for one-step delay compensation, and to simultaneously estimate the model parameter disturbance. The estimated disturbance of this observer is used to estimate the stator resistance offline. Then the estimated resistance is required to update the designed sliding-mode observer, which can be used to estimate the inductance and permanent-magnetic flux linkage online. In addition, the flux and torque estimation of the next control period, which is unaffected by the model parameter disturbance, is achieved by using predictive d-q axis currents and estimated parameters. Hence, a low parameter sensitivity DB-DTC method is developed. Simulation and experimental results show the validity of the proposed direct control method.

**Key words:** Deadbeat direct torque control, Observer, Parameter disturbance, Permanent-magnet synchronous motor

## I. INTRODUCTION

In a PMSM drive system, the important consideration that influences the control performance of the drive system is a fast dynamic torque response. Therefore, direct torque control (DTC) is widely applied in machine control systems to improve the torque control capability. In the classic DTC method, the voltage vector applied in the motor is directly selected from a predefined offline state table. It has the advantages of a fast dynamic response and a simple control structure. However, the disadvantage of a large torque ripple and a variable switching frequency cannot be ignored [1]-[3].

As a possible alternative control strategy, deadbeat direct torque control (DB-DTC) is attracting widespread interest. The

DB-DTC method that has a fast dynamic performance and low torque and flux ripples. In addition, it can obtain a desired response in one switching period with a constant switching frequency. The DB-DTC method has been applied for different drive systems, such as permanent-magnet synchronous machine (PMSM) control systems [4]-[6], induction machine control systems [7]-[9] and synchronous reluctance machines drives [10]. However, the deadbeat direct torque control is dependent on an accurate motor model, which means that a model parameter mismatch would make the calculated voltage references deviate from their expected values. Furthermore, the control performance of the DB-DTC method is related to stator flux and torque estimations [11]-[14], which are used as feedback values of the closed loop control. It should be noted that stator flux and torque estimations are also obtained according to the machine model. Therefore, parameter variations have great effect on the control performance of DB-DTC systems [15], [16]. Parameter estimation is very necessary to achieve accurate control of the stator flux and

Manuscript received Apr. 23, 2017, 2017; accepted Jun. 8, 2017

Recommended for publication by Associate Editor Kwang-Woon Lee.

<sup>†</sup>Corresponding Author: zxg@ncut.edu.cn

Tel: +86-010-8880-2691, North China University of Technology

<sup>\*</sup>Collaborative Innovation Center of Key Power Energy-Saving Technologies in Beijing, North China University of Technology, China

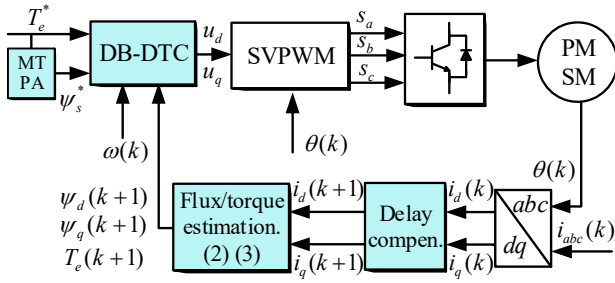


Fig.1. Control diagram of the conventional DB-DTC method.

torque in DB-DTC. Most of the reported methods for parameter estimation are targeted to field-oriented control drives, such as the injection-based method [17], [18], the model reference adaptive system based method [19], [20] and extended Kalman filters [21], [22].

However, many methods have been published recently for solving the parameter variation problems in DB-DTC [23]-[25]. In [23], two kinds of parameter estimation methods, i.e., a flux observer-based model reference adaptive system and a pulsating flux injection-based method, are developed and integrated on a deadbeat direct torque and flux control system. Experimental results show the validity of both methods. In [24], in order to compensate variations of the motor parameters, a predictive control method with a parallel integral loop is investigated. To obtain an accurate stator flux and torque estimation under the condition of model parameter variations, an inductance estimation method based on high-frequency injection is presented in [25] for the application of deadbeat direct torque and flux control. Moreover, the stator resistance and permanent-magnet flux linkage are estimated based on the recursive least squares method. In this method, the estimated parameters are used for designing the stator flux linkage and torque observer, which improve the performance of the torque/flux estimation and system control. The aforementioned estimation methods are able to provide precise values for the parameter estimation and to reduce control sensitivity to parameter variations. However, it is difficult to use these methods to simultaneously estimate the model parameters and predict the stator currents used for the delay compensation in the digital control due to a lack of model predictive capability.

In this paper, an improved deadbeat direct torque control method for SPMSM drives is proposed. First, the track errors of the stator flux and torque that are caused by model parameter variations are analyzed. Then an observer that can predict the d-q axis currents of the next control period, which are used for one-step delay compensation and to simultaneously estimate the model parameter disturbance caused by parameter variations, is designed. The estimated parameter disturbances are used for estimating the stator resistance offline. Then the inductance and permanent-magnetic flux linkage are estimated online based on a resistance-updated observer and a designed sliding-mode adaptive law, respectively. In addition, based on the predictive

d-q axis currents and estimated parameters, the flux and torque estimation of the next control period that is unaffected by model parameter disturbances is achieved. They are then used as the feedback of the system. Hence, a law parameter sensitivity DB-DTC method is developed. Finally, simulation and experimental results show the validity of the proposed direct control method.

## II. SPMSM MODEL

The model of the SPMSM is given as:

$$\begin{cases} u_d = Ri_d - \omega\psi_q + \frac{d\psi_d}{dt} \\ u_q = Ri_q + \omega\psi_d + \frac{d\psi_q}{dt} \end{cases} \quad (1)$$

The flux linkage equations are expressed as follows:

$$\begin{cases} \psi_d = Li_d + \psi_f \\ \psi_q = Li_q \end{cases} \quad (2)$$

The electromagnetic torque equation is:

$$T_e = 1.5p\psi_f i_q \quad (3)$$

In this model,  $u_d$  and  $u_q$  are the d-axis and q-axis stator voltages,  $i_d$  and  $i_q$  are the d-axis and q-axis stator currents,  $\psi_d$  and  $\psi_q$  are the d-axis and q-axis flux linkage,  $L_d=L_q=L$  represents the inductance,  $R$  represents the resistance, and  $\psi_f$  and  $\omega$  are the permanent magnet flux linkage and angular velocity, respectively.

## III. DEADBEAT DIRECT TORQUE CONTROL

A control diagram of the PMSM deadbeat direct torque control is illustrated in Fig. 1. The voltage vectors ( $u_d$  and  $u_q$ ) are calculated based on the DB-DTC algorithm, which is introduced in session A. Then this voltage vector is converted to switching signals through SVPWM. The delay compensation part is used to compensate the one-step control delay in the digital control. The torque reference command can be obtained from the output of the speed PI controller, and the reference command of the stator flux is computed by the MTPA algorithm based on the torque reference value, i.e.,

$$\psi_s^* = \sqrt{\psi_f^2 + [LT_e^*/(1.5p\psi_f)]^2}. \quad \text{Details of the conventional}$$

deadbeat direct torque control system are introduced in the following section.

### A. Deadbeat Direct Torque Control Algorithm

According to voltage equation (1) and flux linkage equation (2), the following discrete expression can be obtained:

$$\begin{cases} \psi_d(k+1) = T_s u_d(k) + \psi_d(k) + T_s \omega(k) \psi_q(k) - \frac{T_s R}{L} [\psi_d(k) - \psi_f] \\ \psi_q(k+1) = T_s u_q(k) + \psi_q(k) - T_s \omega(k) \psi_d(k) - \frac{T_s R}{L} \psi_q(k) \end{cases} \quad (4)$$

where  $T_s$  is a sampling period. Next, substituting the  $q$  axis

flux (2) into (3) yields:

$$T_e = \frac{3}{2} p \psi_f \frac{\psi_q}{L} \quad (5)$$

Taking the time derivative of the torque, the following discrete expression can be obtained:

$$T_e(k+1) - T_e(k) = \frac{3}{2} p \frac{\psi_f}{L} [\psi_q(k+1) - \psi_q(k)] \quad (6)$$

Then according to (4) and (6), the relation between the torque and the q axis voltage can be shown in (7).

$$u_q(k) T_s = B \quad (7)$$

$$\text{where } B = \frac{2L}{3p\psi_f} [T_e(k+1) - T_e(k)] + \frac{T_s R \psi_q(k)}{L} + T_s \omega(k) \psi_d(k)$$

In addition, based on (4), the relation of the stator flux and the stator voltage can be obtained:

$$\begin{aligned} \psi_s^2(k+1) &= \psi_d^2(k+1) + \psi_q^2(k+1) \\ &= [T_s u_d(k) + \psi_d(k) + T_s \omega(k) \psi_q(k) - \frac{T_s R}{L} (\psi_d(k) - \psi_f)]^2 \\ &\quad + [T_s u_q(k) + \psi_q(k) - T_s \omega(k) \psi_d(k) - \frac{T_s R}{L} \psi_q(k)]^2 \end{aligned} \quad (8)$$

In deadbeat direct torque control, to implement satisfactory torque and stator flux performance in the next control period, the torque and stator flux of the next control period, i.e.,  $T_e(k+1)$  and  $\psi_s(k+1)$ , need to be selected as reference commands. This means that  $T_e^* = T_e(k+1)$  and  $\psi_s^* = \psi_s(k+1)$ . Then from (7) and (8), the stator voltage of the motor that allows the actual torque and stator flux to reach their reference values after a modulation period can be obtained as follows [3][6]:

$$\begin{cases} u_d(k) = \frac{-X_1 + \sqrt{X_1^2 - X_2}}{T_s} \\ u_q(k) = \frac{B}{T_s} \end{cases} \quad (9)$$

where:

$$\begin{aligned} X_1 &= \psi_d(k) + T_s \omega(k) \psi_q(k) - \frac{T_s R}{L} [\psi_d(k) - \psi_f] \\ X_2 &= B^2 + 2B[\psi_q(k) - T_s \omega(k) \psi_d(k) - \frac{T_s R}{L} \psi_q(k)] \\ &\quad + [1 + T_s^2 \omega^2(k) - \frac{2T_s R}{L} + \frac{T_s^2 R^2}{L^2}] [\psi_d^2(k) + \psi_q^2(k)] \\ &\quad + \frac{T_s R}{L} \psi_f [\frac{T_s R}{L} \psi_f + 2\psi_d(k) + 2T_s \omega(k) \psi_q(k) - \frac{2T_s R}{L} \psi_d(k)] - (\psi_s^*)^2 \\ B &= \frac{2L}{3p\psi_f} [T_e^* - T_e(k)] + \frac{T_s R \psi_q(k)}{L} + T_s \omega(k) \psi_d(k). \end{aligned}$$

### B. One-step Delay Compensation

In real applications, the computed voltage vector in the present period is applied until the next period. Therefore, the one-step control delay exists between the applied voltage vector and the computed voltage vector. This delay, which is

caused by digital implementation, can deteriorate the performance of the PMSM system if it is not considered in the design of the controller. The negative impact of the one-step delay is especially serious when the sampling frequency is low. Therefore, in order to improve the control performance, one-step delay compensation is necessary. In this paper, the predictive currents at the (k+1)th instant can be obtained based on the Euler-forward discretization method, which is expressed as:

$$\begin{cases} i_d(k+1) = i_d(k) + \frac{T_s}{L} (u_d(k) - R_s i_d(k) + \omega L_q i_q(k)) \\ i_q(k+1) = i_q(k) + \frac{T_s}{L} (u_q(k) - R_s i_q(k) - \omega L_d i_d(k) - \omega \psi_f) \end{cases} \quad (10)$$

Then the sampled currents can be replaced by predictive currents  $i_d(k+1)$  and  $i_q(k+1)$  to compensate the one-step control delay. Therefore, the torque and stator flux observer, which is based on the electromagnetic torque (3) and stator flux (2), can be designed to implement the torque and stator flux estimation at the (k+1)th instant by the following expression:

$$\begin{cases} \psi_d(k+1) = L i_d(k+1) + \psi_f \\ \psi_q(k+1) = L i_q(k+1) \end{cases} \quad (11)$$

$$T_e(k+1) = \frac{3}{2} p \psi_f i_q(k+1) \quad (12)$$

## IV. PARAMETER SENSITIVITY ANALYSIS OF THE DEADBEAT DIRECT TORQUE CONTROL

The deadbeat direct torque control is a model-based control method because three machine parameters (stator inductance, stator resistance and permanent magnetic flux linkage) are included in (9), which means this control method is parameter sensitive. In addition, the stator flux and torque estimation needs a precise stator inductance and permanent magnetic flux linkage. In other words, the accuracy of the machine model directly influences the control performance of the whole system. In order to evaluate how sensitive the deadbeat direct torque control is to parameter variations, a parameter sensitivity analysis is discussed in this section.

In a practical control system, a deadbeat direct torque controller calculates the voltage vector in the current control period based on (9). This means that the actual torque and stator flux of the PMSM can reach the reference values of the torque and stator flux after a modulation period without the dc bus limitation. However, it should be noted that equation (9) of the deadbeat direct torque control includes motor parameters ( $R$ ,  $L$  and  $\psi_f$ ), which are crude estimations of the true values. These crude estimation values can be initially obtained by prior knowledge. Next, the calculated voltage vector based on (9) should be applied to the real PMSM system by SVPWM. Then the torque response and stator flux response can be observed. This process is described in (13),

where  $R_0$ ,  $L_0$  and  $\psi_{f0}$  are the true parameter values, and  $\psi_{d0}(k)$  and  $\psi_{q0}(k)$  can be expressed as  $\psi_{d0}(k) = L_{d0}i_d(k) + \psi_{f0}$ ,  $\psi_{q0}(k) = L_{q0}i_q(k)$ .

$$\begin{cases} \psi_{d0}(k+1) = T_s u_d(k) + \psi_{d0}(k) + T_s \omega(k) \psi_{q0}(k) - \frac{T_s R_0}{L_0} [\psi_{d0}(k) - \psi_{f0}] \\ \psi_{q0}(k+1) = T_s u_q(k) + \psi_{q0}(k) - T_s \omega(k) \psi_{d0}(k) - \frac{T_s R_0}{L_0} \psi_{q0}(k) \end{cases} \quad (13)$$

Thus, substituting (9) into (13), the following equations can be obtained:

$$\psi_d(k+1) = \psi_d^*(k+1) + (T_s \Delta R - \Delta L) i_d(k) - \Delta L T_s \omega_e(k) i_q(k) - \Delta \psi_f \quad (14)$$

$$\psi_q(k+1) = \psi_q^*(k+1) + (T_s \Delta R - \Delta L) i_q(k) - \Delta L T_s \omega_e(k) i_d(k) + T_s \Delta \psi_f \omega_e(k) \quad (15)$$

where  $\Delta R = R - R_0$ ,  $\Delta L = L - L_0$  and  $\Delta \psi_f = \psi_f - \psi_{f0}$  represent the parameter errors between the true values and their crude estimations. According to (5) and (15), the relation between the torque reference and its response can be described as:

$$\begin{aligned} T_e(k+1) &= \frac{\psi_f - \Delta \psi_f}{L - \Delta L} \frac{L}{\psi_f} T_e^*(k+1) + \frac{3}{2} p \frac{\psi_f - \Delta \psi_f}{L - \Delta L} (\Delta R T_s - \Delta L) i_q(k) \\ &\quad - \frac{3}{2} p \frac{\psi_f - \Delta \psi_f}{L - \Delta L} \Delta L T_s \omega_e(k) i_d(k) + \frac{3}{2} p \frac{\psi_f - \Delta \psi_f}{L - \Delta L} \Delta \psi_f T_s \omega_e(k) \end{aligned} \quad (16)$$

From (14), (15) and (16), it can be seen that the existence of the parameter variation or error influences the track performance of the torque and stator flux.

In addition, it should be noted that the one-step delay needs to be compensated based on (10), (11) and (12) in real applications. Therefore, the voltage output (9) of DB-DTC has a different form.

$$\begin{cases} u'_d(k+1) = \frac{-X'_1 + \sqrt{X_1'^2 - X_2'^2}}{T_s} \\ u'_q(k+1) = \frac{B'}{T_s} \end{cases} \quad (17)$$

where:

$$B' = \frac{2L}{3p\psi_f} [T_e^* - T_e(k+1)] + \frac{T_s R \psi_q(k+1)}{L} + T_s \omega(k) \psi_d(k+1)$$

$$X_1' = \psi_d(k+1) + T_s \omega(k) \psi_q(k+1) - \frac{T_s R}{L} [\psi_d(k+1) - \psi_f]$$

$$X_2' = B'^2 + 2B'[\psi_q(k+1) - T_s \omega(k) \psi_d(k+1) - \frac{T_s R}{L} \psi_q(k+1)]$$

$$+ [1 + T_s^2 \omega^2(k) - \frac{2T_s R}{L} + \frac{T_s^2 R^2}{L^2}] [\psi_d^2(k+1) + \psi_q^2(k+1)]$$

$$+ \frac{T_s R}{L} \psi_f [\frac{T_s R}{L} \psi_f + 2\psi_d(k+1) + 2T_s \omega(k) \psi_q(k+1)]$$

$$- \frac{2T_s R}{L} \psi_d(k+1) - (\psi_s^*)^2.$$

The variables  $\psi_d(k+1)$ ,  $\psi_q(k+1)$  and  $T_e(k+1)$  in (17) are obtained based on the one-step compensation equations (10), (11) and (12). Similarly, substituting (17) into (13), the following equations can be obtained:

$$\psi_d(k+2) = \psi_d^*(k+2) + (T_s \Delta R - \Delta L) i_d(k+1) - \Delta L T_s \omega_e(k) i_q(k+1) - \Delta \psi_f \quad (18)$$

$$\psi_q(k+2) = \psi_q^*(k+2) + (T_s \Delta R - \Delta L) i_q(k+1) - \Delta L T_s \omega_e(k) i_d(k+1) + T_s \Delta \psi_f \omega_e(k) \quad (19)$$

In (18) and (19), both of the compensated currents, i.e.,  $i_d(k+1)$  and  $i_q(k+1)$ , are not accurate current values of the next control period due to the existence of parameter disturbances, which can be expressed using accurate values of the currents and parameter disturbances, as shown as (20).

$$\begin{cases} i_d(k+1) = i_d(k) + \frac{T_s}{L} (u_d(k) - R_s i_d(k) + \omega L_q i_q(k)) \\ \quad = i_{d0}(k+1) + T_s f'_d \\ i_q(k+1) = i_q(k) + \frac{T_s}{L} (u_q(k) - R_s i_q(k) - \omega L_d i_d(k) - \omega \psi_f) \\ \quad = i_{q0}(k+1) + T_s f'_q \end{cases} \quad (20)$$

where  $i_{d0}(k+1)$  and  $i_{q0}(k+1)$  represent accurate current values, and  $f'_d$  and  $f'_q$  represent parameter disturbances, which can be expressed as:

$$\begin{cases} f'_d = u_d(k) \left( \frac{1}{L - \Delta L} - \frac{1}{L} \right) + i_d(k) \left( \frac{R}{L} - \frac{R - \Delta R}{L - \Delta L} \right) \\ f'_q = u_q(k) \left( \frac{1}{L} - \frac{1}{L - \Delta L} \right) + i_q(k) \left( \frac{R - \Delta R}{L - \Delta L} - \frac{R}{L} \right) \\ \quad + \omega_e(k) \left( \frac{\psi_f - \Delta \psi_f}{L - \Delta L} - \frac{\psi_f}{L} \right) \end{cases} \quad (21)$$

Substituting (20) into (18) and (19), the stator flux responses of the control system can be obtained as follows:

$$\psi_d(k+2) = \psi_d^*(k+2) + (T_s \Delta R - \Delta L) [i_{d0}(k+1) + T_s f'_d] - \Delta L T_s \omega_e(k) [i_{q0}(k+1) + T_s f'_q] - \Delta \psi_f \quad (22)$$

$$\psi_q(k+2) = \psi_q^*(k+2) + (T_s \Delta R - \Delta L) [i_{q0}(k+1) + T_s f'_q] - \Delta L T_s \omega_e(k) [i_{d0}(k+1) + T_s f'_d] + T_s \Delta \psi_f \omega_e(k) \quad (23)$$

Similarly, the torque responses can be derived by:

$$\begin{aligned} T_e(k+2) &= \frac{L}{L - \Delta L} \frac{\psi_f - \Delta \psi_f}{\psi_f} T_e^*(k+2) + \frac{3}{2} p (\Delta R T_s - \Delta L) [i_{q0}(k+1) + T_s f'_q] \\ &\quad - \frac{3}{2} p \Delta L T_s \omega_e(k) [i_{d0}(k+1) + T_s f'_d] + \frac{3}{2} p \Delta \psi_f T_s \omega_e(k) \end{aligned} \quad (24)$$

From (22), (23) and (24), it can be seen that the conventional one-step delay compensation is not accurate due to model parameter disturbances, which further deteriorates the track performance of the torque and stator flux.

Therefore, in order to improve the performance of PMSM deadbeat direct torque control systems, it is necessary to develop a low parameter sensitivity control algorithm.

## V. LOW PARAMETER SENSITIVITY DEADBEAT DIRECT TORQUE CONTROL

In order to improve the control performance of a deadbeat direct torque control system, a low parameter sensitivity deadbeat direct torque control method is proposed. This method can be implemented in two steps. Step 1 is performed to estimate resistance offline. Step 2 is performed to estimate inductance/permanent-magnet flux linkage online, and to implement the proposed control algorithm. A control diagram of the proposed method is shown in Fig. 2.

Firstly, an observer that can predict the stator current of the next control period and simultaneously track parameter disturbances is introduced. Then the resistance can be estimated offline according to the estimated parameter disturbance of the observer. The estimated resistance is used to update this observer. Then the stator inductance and permanent-magnet flux linkage are estimated online using the estimated parameter disturbance of the d-axis and sliding-mode adaptive law, respectively. Based on the estimated motor parameters and predictive currents of the observer, i.e.,  $\hat{i}_d(k+1)$  and  $\hat{i}_q(k+1)$ , an accurate one-step delay compensation can be achieved and the tracking error caused by parameter disturbances can be eliminated.

This section is arranged as follows. Subsection A introduces a novel observer. The estimations of the resistance, permanent-magnetic flux linkage and inductance are described in subsections B, C and D, respectively. Finally, low parameter sensitivity deadbeat direct torque control method is presented in subsection E.

### A. Observer

Based on motor models (1) and (2), the four-order state equation of a SPMSM can be described as follows, when the parameters variations are taken into consideration:

$$\frac{d}{dt} \begin{bmatrix} i_s \\ f_s \end{bmatrix} = \begin{bmatrix} A_{11} & A_{12} \\ 0 & 0 \end{bmatrix} \begin{bmatrix} i_s \\ f_s \end{bmatrix} + \begin{bmatrix} B \\ 0 \end{bmatrix} u_s + \begin{bmatrix} C \\ 0 \end{bmatrix} \quad (25)$$

where:

$$A_{11} = \begin{bmatrix} -\frac{R}{L} & \omega \\ -\omega & -\frac{R}{L} \end{bmatrix} \quad A_{12} = \begin{bmatrix} -\frac{1}{L} & 0 \\ 0 & -\frac{1}{L} \end{bmatrix} \quad B = \begin{bmatrix} \frac{1}{L} & 0 \\ 0 & \frac{1}{L} \end{bmatrix}$$

$$C = \begin{bmatrix} 0 \\ -\frac{\omega}{L} \psi_f \end{bmatrix} \quad u_s = \begin{bmatrix} u_d \\ u_q \end{bmatrix} \quad i_s = \begin{bmatrix} i_d \\ i_q \end{bmatrix} \quad f_s = \begin{bmatrix} f_d \\ f_q \end{bmatrix}$$

In (25),  $u_s$  is the measured voltage, and  $f_d$  and  $f_q$  represent the parameter disturbances, which are described in (26) and (27).

$$f_d = \Delta L \frac{di_d}{dt} + \Delta R i_d - \Delta L \omega i_q \quad (26)$$

$$f_q = \Delta L \frac{di_q}{dt} + \Delta R i_q + \Delta L \omega i_d + \Delta \psi_f \omega \quad (27)$$

According to (25), a sliding-mode style observer is designed to simultaneously estimate the stator currents at the next

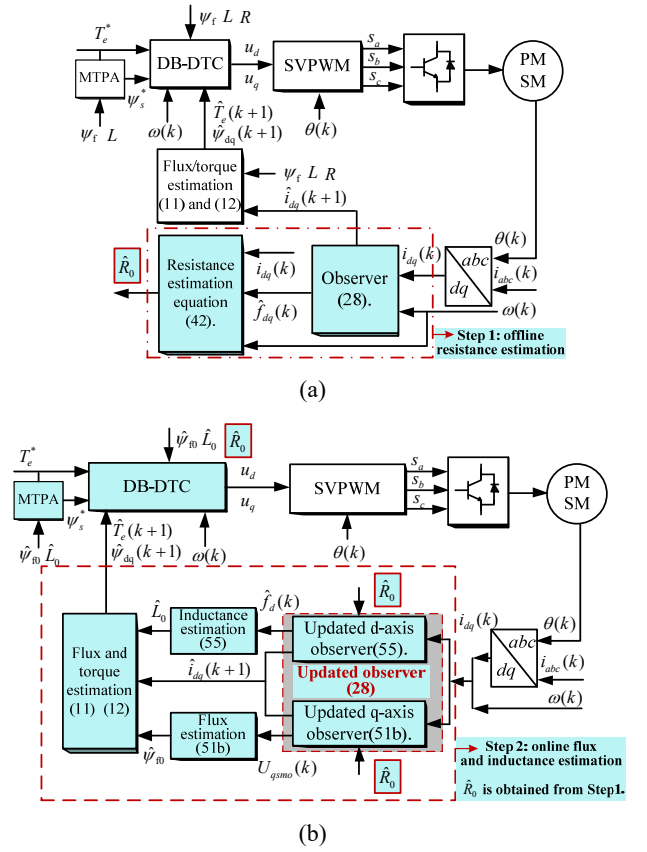


Fig. 2. Control diagrams of the proposed low parameter sensitivity DB-DTC method. (a) Step 1: offline resistance estimation. (b) Step 2: online inductance and flux linkage estimation and algorithm implementation.

control period and the parameter disturbances, which is shown as follows:

$$\frac{d}{dt} \begin{bmatrix} \hat{i}_s \\ \hat{f}_s \end{bmatrix} = \begin{bmatrix} A_{11} & A_{12} \\ 0 & 0 \end{bmatrix} \begin{bmatrix} \hat{i}_s \\ \hat{f}_s \end{bmatrix} + \begin{bmatrix} B \\ 0 \end{bmatrix} u_s + \begin{bmatrix} A_{12} \\ D \end{bmatrix} U_{smo} + \begin{bmatrix} C \\ 0 \end{bmatrix} \quad (28)$$

where:

$$D = \begin{bmatrix} \mu_d & 0 \\ 0 & \mu_q \end{bmatrix} \quad U_{smo} = \begin{bmatrix} U_{dsmo} \\ U_{qsmo} \end{bmatrix}$$

In (28),  $U_{dsmo}$  and  $U_{qsmo}$  represent sliding-mode control functions, which are discussed below. The error equation between the motor model (25) and the observer (28) can be computed as:

$$\frac{d}{dt} \begin{bmatrix} e_i \\ e_f \end{bmatrix} = \begin{bmatrix} A_{11} & A_{12} \\ 0 & 0 \end{bmatrix} \begin{bmatrix} e_i \\ e_f \end{bmatrix} + \begin{bmatrix} A_{12} \\ D \end{bmatrix} U_{smo} \quad (29)$$

where:

$$e_i = \begin{bmatrix} e_{id} \\ e_{iq} \end{bmatrix} = \begin{bmatrix} \hat{i}_d - i_d \\ \hat{i}_q - i_q \end{bmatrix} \quad e_f = \begin{bmatrix} e_{fd} \\ e_{fq} \end{bmatrix} = \begin{bmatrix} \hat{f}_d - f_d \\ \hat{f}_q - f_q \end{bmatrix}$$

In order to ensure that the stator current estimation errors and parameter disturbance estimation errors quickly converge to zero, the sliding-mode control function  $U_{smo}$  should be reasonably designed. In this paper, the reaching law based

design method is adopted. Firstly, an easy linear sliding-mode surface is designed as:

$$s = \begin{bmatrix} s_d \\ s_q \end{bmatrix} = \begin{bmatrix} e_{id} \\ e_{iq} \end{bmatrix} = \begin{bmatrix} \hat{i}_d - i_d \\ \hat{i}_q - i_q \end{bmatrix} \quad (30)$$

Then the equal speed sliding mode reaching law (31) is introduced to design the sliding mode control function.

$$\frac{ds}{dt} = -k \cdot \text{sign}(s) \quad (31)$$

where  $k$  is the positive reaching coefficient.

According to (29), (30) and (31), considering  $e_f$  as a disturbance, the expression of the sliding-mode control function can be derived as:

$$U_{smo} = A_{11}e_i + k \cdot \text{sign}(e_i) \quad (32)$$

The proposed observer, which is controlled by the designed control function (32), should be able to guarantee the convergence of  $e_i$  and  $e_f$ . This means that the sliding-mode stability condition (33) must be satisfied.

$$\begin{cases} \dot{V}_d = s_d \cdot \dot{s}_d = e_{\psi d} \cdot \dot{e}_{\psi d} \leq 0 \\ \dot{V}_q = s_q \cdot \dot{s}_q = e_{\psi q} \cdot \dot{e}_{\psi q} \leq 0 \end{cases} \quad (33)$$

Substituting (29) and (32) into (33), yields:

$$\begin{aligned} \dot{V}_d &= e_{id} \left( -\frac{R}{L} e_{id} + \omega e_{iq} - \frac{1}{L} e_{fd} - \frac{1}{L} U_{dsmo} \right) \\ &= -e_{id} \left[ -\frac{1}{L} e_{fd} - k \cdot \text{sign}(e_{id}) \right] \leq 0 \end{aligned} \quad (34)$$

$$\begin{aligned} \dot{V}_q &= e_{iq} \left( -\frac{R}{L} e_{iq} - \omega e_{\psi d} - e_{fq} - U_{qsmo} \right) \\ &= -e_{iq} \left[ -\frac{1}{L} e_{fq} - k \cdot \text{sign}(e_{iq}) \right] \leq 0 \end{aligned} \quad (35)$$

Therefore, the parameter  $k$  should be selected according to the following expression to guarantee the stability of the sliding mode observer.

$$k > \max \left( \frac{|e_{fd}|}{L}, \frac{|e_{fq}|}{L} \right). \quad (36)$$

Under the action of the control function  $U_{smo}$  with parameter  $k$ , this observer reaches the sliding-mode surface in a finite amount of time and stays on it. This means that the error values  $e_{id}$  and  $e_{iq}$  along with their derivatives  $\dot{e}_{id}$  and  $\dot{e}_{iq}$  can converge to zero. Substituting the expressions  $e_{id} = e_{iq} = 0$  and  $\dot{e}_{id} = \dot{e}_{iq} = 0$  into (29) yields:

$$\frac{de_f}{dt} + De_f = 0 \quad (37)$$

Solving (37) yields:

$$\begin{cases} e_{fd} = C \cdot e^{-\mu_d t} \\ e_{fq} = C \cdot e^{-\mu_q t} \end{cases} \quad (38)$$

where  $C$  is a constant. Equation (38) indicates that the positive or negative sign and parameter amplitude of  $\mu_d$  and  $\mu_q$  both have an important influence on the convergence of

the errors  $e_{fd}$  and  $e_{fq}$ . Therefore, the positive  $\mu_d$  and  $\mu_q$  must be used to guarantee the convergence.

### B. Resistance Estimation

According to above analysis, it can be seen that this observer is stable when appropriate parameters (including  $k$ ,  $\mu_d$  and  $\mu_q$ ) are determined. Therefore, the parameter disturbance information  $f_d$  and  $f_q$  can be observed exactly. This means that the electrical parameters of the motor can be extracted from these disturbances based on (26) and (27). Detailed information of the resistance estimation is described in the following text.

The estimated resistance satisfying  $\hat{R}_0 = R - \Delta \hat{R}$ , in which the crude estimation of the resistance, i.e.,  $R$ , is known as the initial value. This means that the estimated value of the true resistance can be obtained by the estimating error  $\Delta R$ . At the stage of the estimating resistance (Step 1), the SPMSM should be operated under two different operation conditions (different current or speed). According to the observer and the q-axis disturbance expression (27), the items  $\Delta L \frac{di_q}{dt}$  and

$\Delta L \omega i_d$  can be ignored under the MTPA control of the

SPMSM at the steady state, i.e.,  $\frac{di_q}{dt} \approx 0$  and  $i_d \approx 0$ . Thus, the estimation value of the q-axis disturbance in the first operation condition can be described as:

$$f_{q1} = \Delta R i_{q1} + \Delta \psi_f \omega_1 \quad (39)$$

Under the second operation condition, the expression of the estimated q-axis disturbance is shown as:

$$f_{q2} = \Delta R i_{q2} + \Delta \psi_f \omega_2 \quad (40)$$

Subtracting (39) from (40), yields:

$$\Delta \hat{R} = \frac{\omega_1 f_{q2} - \omega_2 f_{q1}}{i_{q2} \omega_1 - i_{q1} \omega_2} \quad (41)$$

Thus, the estimated stator resistance is obtained as:

$$\hat{R}_0 = R - \frac{\omega_1 f_{q2} - \omega_2 f_{q1}}{i_{q2} \omega_1 - i_{q1} \omega_2} \quad (42)$$

### C. Permanent-Magnet Flux Linkage Estimation

In a DB-DTC system, except for the resistance  $R$ , accurate parameters  $L$  and  $\psi_f$  are important. They determine the control performance of the whole control system, because they exist in the system reference, feedback and controller, i.e., the flux reference MTPA, the stator flux/torque estimation (11) (12) and the solution of the DB-DTC (9). Therefore, the online estimation of the inductance and permanent-magnet flux linkage is necessary. This subsection discusses the estimation of the permanent-magnet flux linkage based on the updated q-axis observer of the observer (28). The estimation of stator the inductance will be discussed in next subsection.

After estimating stator resistance, the initial value  $R$  in (28) can be updated by  $\hat{R}_0$ . Therefore, the q-axis observer of the observer (28) can be updated as:

$$\begin{cases} L \frac{d\hat{i}_q}{dt} = u_q - \hat{R}_0 \hat{i}_q - \omega L i_d - \omega \hat{\psi}_{f0} - \hat{f}_q - U_{qsmo} \\ \frac{d\hat{f}_q}{dt} = \mu_q U_{qsmo} \end{cases} \quad (43)$$

where  $\hat{\psi}_{f0} = \psi_{f0} - \Delta\psi_f$  represents the estimated permanent-magnet flux linkage. The error equation between the motor model (25) and the updated q-axis observer (43) is derived as:

$$\begin{cases} \frac{de_{iq}}{dt} = -\frac{R_0}{L} e_{iq} - \frac{\omega}{L} \Delta\psi_f - \frac{1}{L} e_{iq} - \frac{1}{L} U_{qsmo} \\ \frac{de_{f_q}}{dt} = \mu_q U_{qsmo} \end{cases} \quad (44)$$

Under the action of the control function  $U_{qsmo}$ , the error  $e_{iq}$  and its derivative  $\dot{e}_{iq}$  can converge to zero. Thus, (44) can be simplified as:

$$\begin{cases} e_{iq} = -\omega \Delta\psi_f - U_{qsmo} \\ \frac{de_{iq}}{dt} = \mu_q U_{qsmo} \end{cases} \quad (45)$$

In order to estimate the parameter  $\psi_f$  exactly, a Lyapunov function is designed as follows:

$$V = \frac{1}{2} e_{iq}^2 + \frac{1}{2} \frac{\Delta\psi_f^2}{b} \quad (46)$$

where  $b$  is the adjusting coefficient. Calculating the derivative of (46), yields:

$$\dot{V} = e_{iq} \dot{e}_{iq} + \frac{\Delta\psi_f}{b} \Delta\dot{\psi}_f \quad (47)$$

According to (47), it can be seen that the error  $e_{iq}$  and  $\Delta\psi_f$  can converge to zero at the same time, when  $\dot{V} \leq 0$  is guaranteed.

Substituting (45) into (47), yields:

$$\dot{V} = -\mu_q U_{qsmo}^2 - \omega \Delta\psi_f \mu_q U_{qsmo} + \frac{\Delta\psi_f}{b} \Delta\dot{\psi}_f \quad (48)$$

To ensure that (48) is less than 0, the following equation should be satisfied, because the item of  $-\mu_q U_{qsmo}^2$  is negative number.

$$-\omega \Delta\psi_f \mu_q U_{qsmo} + \frac{\Delta\psi_f}{b} \Delta\dot{\psi}_f = 0 \quad (49)$$

Therefore, the adaptive law of the permanent-magnet flux linkage estimation can be designed as follows:

$$\dot{\hat{\psi}}_{f0} = \frac{d(\hat{\psi}_{f0} - \psi_{f0})}{dt} = -\Delta\dot{\psi}_f = -b\omega\mu_q U_{qsmo} \quad (50)$$

With this adaptive law, the q-axis observer, which can predict the q-axis current of the next control period ( $\hat{i}_q(k+1)$ ) and simultaneously estimate the permanent-magnet flux linkage, is described below, and its discrete form is shown in (51b).

$$\begin{cases} L \frac{d\hat{i}_q}{dt} = u_q - R_0 \hat{i}_q - \omega L i_d - \omega \hat{\psi}_{f0} - \hat{f}_q - U_{qsmo} \\ \frac{d\hat{f}_q}{dt} = \mu_q U_{qsmo} \\ \frac{d\hat{\psi}_{f0}}{dt} = -b\omega\mu_q U_{qsmo} \end{cases} \quad (51a)$$

$$\begin{cases} \hat{i}_q(k+1) = (1 - \frac{T_s R}{L}) \hat{i}_q(k) - \omega(k) T_s i_d(k) - \omega(k) \frac{T_s}{L} \hat{\psi}_{f0}(k) \\ \quad + \frac{T_s}{L} [u_q(k) - \hat{f}_q(k) - U_{qsmo}(k)] \\ \hat{f}_q(k+1) = \hat{f}_q(k) + \mu_q T_s U_{qsmo}(k) \\ \hat{\psi}_{f0}(k+1) = \hat{\psi}_{f0}(k) - b\mu_q T_s \omega(k) U_{qsmo}(k) \end{cases} \quad (51b)$$

#### D. Stator Inductance Estimation

On the other hand, after estimating the stator resistance, according to (28), the updated d-axis observer can be obtained as:

$$\begin{cases} L \frac{d\hat{i}_d}{dt} = u_d - \hat{R}_0 \hat{i}_d + \omega L i_q - \hat{f}_d - U_{dsmo} \\ \frac{d\hat{f}_d}{dt} = \mu_d U_{dsmo} \end{cases} \quad (52)$$

It should be noted that  $f_d$  in (52) can be simplified as (53) according to (26), because the item  $\Delta L \frac{di_d}{dt}$  and  $\Delta R i_d$  can be ignored under the MTPA control of the SPMSM in the steady state, i.e.,  $i_d \approx 0$ ,  $\frac{di_d}{dt} \approx 0$  and  $\Delta R \approx 0$ .

$$f_d = -\Delta L \omega i_q \quad (53)$$

Therefore, the stator inductance can be estimated by the following equation:

$$\hat{L}_0 = L + \frac{\hat{f}_d}{\omega i_q} \quad (54)$$

In practical applications, the d-axis observer can be implemented in the following discrete form:

$$\begin{cases} \hat{i}_d(k+1) = (1 - \frac{T_s R}{L}) \hat{i}_d(k) + \omega(k) T_s i_q(k) \\ \quad + \frac{T_s}{L} [u_d(k) - \hat{f}_d(k) - U_{dsmo}(k)] \\ \hat{f}_d(k+1) = \hat{f}_d(k) + \mu_d T_s U_{dsmo}(k) \\ \hat{L}_0(k+1) = L + \hat{f}_d(k) / \omega(k) i_q(k) \end{cases} \quad (55)$$

According to (51) and (55), it can be found that this observer is able to predict the d-q axis currents of the next control period used for the delay compensation and simultaneously estimate the motor parameters.

#### E. Low Parameter Sensitivity DB-DTC Method

To compensate the one-step delay in the conventional DB-DTC, the motor model needs to predict the current of the

next control period using (10). Then based on (11) and (12), the torque and stator flux are predicted. However, when parameter mismatches exist, the predictive torque and stator flux using the model (10), (11) and (12) leads to prediction errors. This means that an inaccurate stator flux and torque are applied in the control system to compensate for the one-step control delay. In order to accurately compensate the one-step control delay, the predictive stator currents of the proposed observer (51) and (55) ( $\hat{i}_d(k+1)$  and  $\hat{i}_q(k+1)$ ) are adopted to predict the stator flux and torque of the next control period with the estimated inductance and permanent-magnet flux linkage. In addition, according to the stator flux reference (MTPA solution) and the solution of the DB-DTC (9), it is obvious that the existence of parameter variations influence the control performance of the whole system. Therefore, a low parameter sensitivity DB-DTC method that includes three parts, i.e., stator flux reference part, DB-DTC part, stator flux/torque prediction and observer part, is designed, as shown in Fig.2. The proposed method can obtain satisfactory control performance, even in the presence of parameter variations.

In practical applications, step 1 is offline resistance estimation, and this process is shown in Fig. 2(a). After estimating the stator resistance, the initial value  $R$  in the observer (28) can be updated by  $\hat{R}_0$ , which means the d-axis and q-axis observers of the observer (28) can both be updated. Then step 2, i.e., the online inductance and flux estimation, can be implemented, and this process is shown in Fig. 2(b).

## VI. SIMULATION AND EXPERIMENTAL RESULTS

### A. Simulation Results

The proposed low parameter sensitivity DB-DTC method and the conventional DB-DTC method are simulated in simulation software (MATLAB/Simulink) to validate the effectiveness of the proposed method. The real parameters of the machine are listed in Table I, and the sampling frequency is 10kHz.

The results of the estimated resistance are shown in Fig. 3, when a parameter mismatch exists. Fig. 3(a) and (b) show the results of the q-axis current and estimated  $f_q$  under two different test condition, and Fig. 3(c) shows an estimated resistance waveform. From the results of Fig. 3, it can be seen that the estimation result of the stator resistance is satisfying.

In addition, the simulation responses of the torque and stator flux are illustrated in Figs. 4 and 5. From top to bottom, the curves are the stator flux reference and its response, the torque reference and its response, the estimated permanent-magnetic flux linkage, and the estimated inductance. At 0.95s, the external load is suddenly changed from 4N·m to the rated value 6N·m, and at 1.05s this load is removed. Simulation results of the conventional DB-DTC and proposed method under inductance parameter variations

TABLE I  
PARAMETERS OF THE PMSM IN SIMULATION AND EXPERIMENT

Parameter	Description	Value
$L_d, L_q$	d- and q-axes inductances	11mH
$R$	stator phase resistance	3Ω
$n$	rated speed	2000 r/min
$P$	number of pole pairs	3
$J$	rotational inertia	0.00129kg·m <sup>2</sup>
$\psi_f$	flux linkage of permanent magnets	0.24Wb

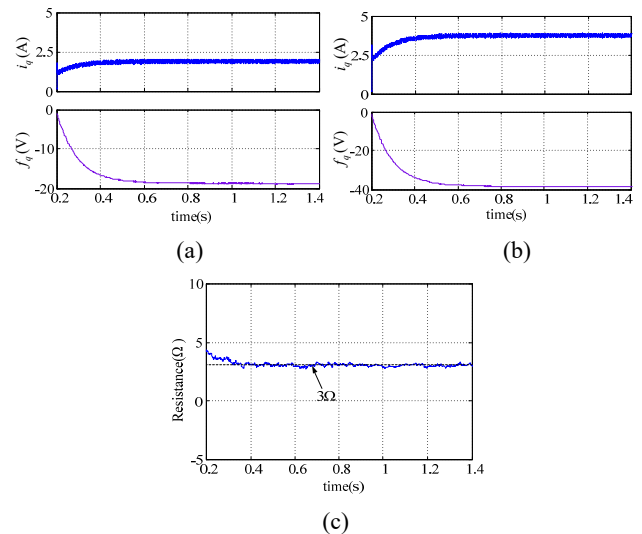


Fig. 3. Simulation results of the stator resistance estimation under  $R=4.3R_0$  at 500r/min: (a) q-axis current and estimated  $f_q$  with a 2N.m load; (b) q-axis current and estimated  $f_q$  with a 4N.m load; (c) estimated stator resistance.

are shown in Fig. 4(a)-(d). In addition, simulation results of both methods under permanent-magnetic flux linkage variations are shown in Fig. 5(a)-(d). It can be seen that the parameter variations have an obviously effect on the track performance of the torque and stator flux, and that the stator flux reference is also influenced. However, it is obvious that the track performances of the torque and stator flux are satisfactory due to the application of the proposed control method. In addition, From Fig. 4(e) and Fig. 5(e), it can be seen that the stator inductance and permanent-magnetic flux linkage can be estimated accurately under different parameter variations, which further demonstrates the validity of the proposed method.

### B. Experimental Results

A 32-bit floating point DSP (TMS320F28335) is used to accomplish the control algorithm development. The PMSM drive platform is shown in Fig. 6. Experimental comparisons between the conventional DB-DTC and the proposed method are carried out and the results are shown in Fig. 7-10.

Fig. 7(a) and (b) show curves of the q-axis current and estimated  $f_q$  under two different test condition, respectively. The estimated stator resistance is shown in Fig. 7(c). These experimental results indicate that accurate resistance



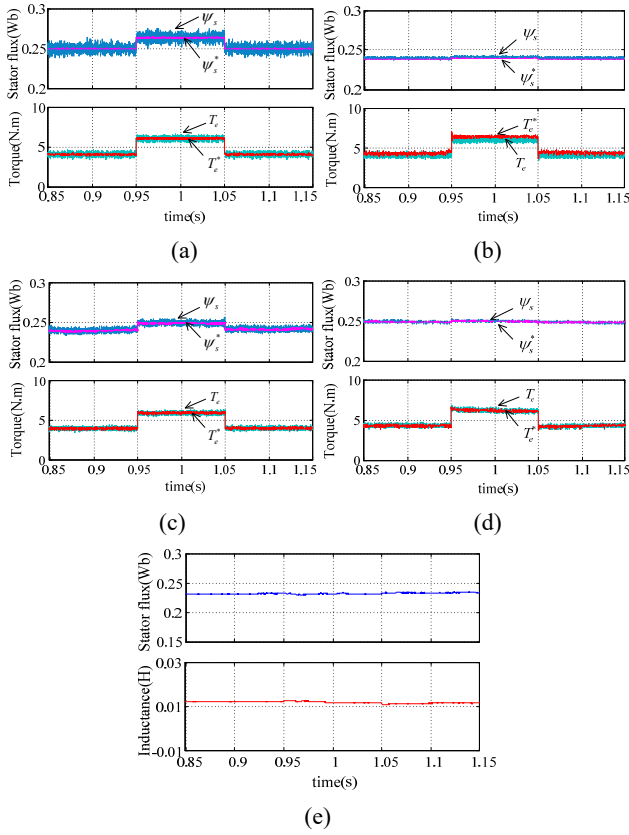


Fig. 4. Simulation results of both methods under  $L=1.5L_0$  and  $L=0.66L_0$  at 500r/min: (a) stator flux and torque response with the DB-DTC method under  $L=1.5L_0$ ; (b) stator flux and torque response with the DB-DTC method under  $L=0.66L_0$ ; (c) stator flux and torque response with the proposed method under  $L=1.5L_0$ ; (d) stator flux and torque response with the proposed method under  $L=0.66L_0$ ; (e) estimation values of the inductance and permanent-magnetic flux linkage using the proposed method.

estimation can be obtained. In addition, when an inductance parameter disturbance exists and the external load of the motor changes from 2 to 4N.m, the stator flux and torque responses of both methods are investigated. The experimental results are shown in Fig. 8. It can be seen that the control performance of the stator flux and torque are not good in the conventional DB-DTC method due to the inductance parameter mismatch ( $L=1.5L_0$ ). However, the proposed method is able to effectively suppress these track errors.

In addition to the inductance parameter disturbance test, a test of the permanent magnet flux linkage variation was also carried out. Fig.9 shows a response comparisons of the stator flux and torque under the conventional DB-DTC and the proposed method with  $\psi_f = 0.5\psi_{f0}$ . It can be seen that the tracking errors caused by the inductance and permanent magnet flux linkage disturbances, which exist in the conventional DB-DTC method, can be effectively compensated using the proposed control method. In addition, from the obtained experimental waveforms, it can be found that the proposed method exhibits much lower stator flux and

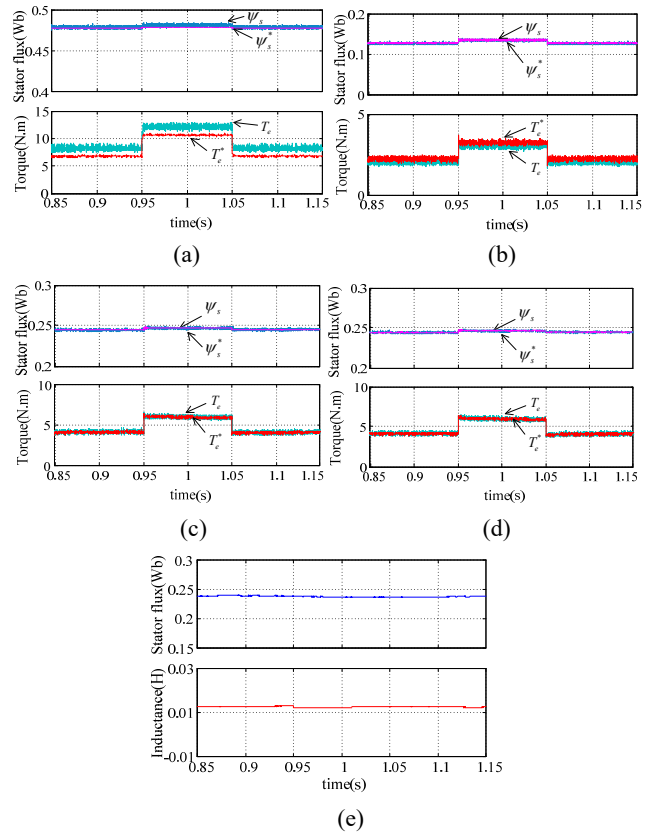


Fig. 5. Simulation results of both methods under  $\psi_f=2\psi_{f0}$  and  $\psi_f=0.5\psi_{f0}$  at 500r/min: (a) stator flux and torque response with the DB-DTC method under  $\psi_f=2\psi_{f0}$ ; (b) stator flux and torque response with the DB-DTC method under  $\psi_f=0.5\psi_{f0}$ ; (c) stator flux and torque response with the proposed method under  $\psi_f=2\psi_{f0}$ ; (d) stator flux and torque response with the proposed method under  $\psi_f=0.5\psi_{f0}$ ; (e) estimation values of the inductance and permanent-magnetic flux linkage using the proposed method.

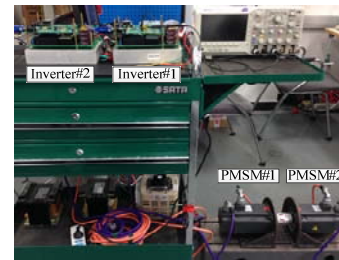


Fig. 6. Experiment platform of a PMSM system.

torque ripples when compared with the conventional DB-DTC method.

Finally, the control performances of both methods are investigated when different parameter disturbances, i.e.  $L=0.66L_0$  and  $\psi_f=2\psi_{f0}$ , coexist in the system. The stator flux and torque response of both methods are displayed in Fig.10 (a)-(d), and the estimated stator inductance, permanent-magnetic flux linkage and estimated disturbances ( $f_d$  and  $f_q$ ) are shown in Fig.10 (e) and (f), respectively. These results indicate that the parameters can be accurately

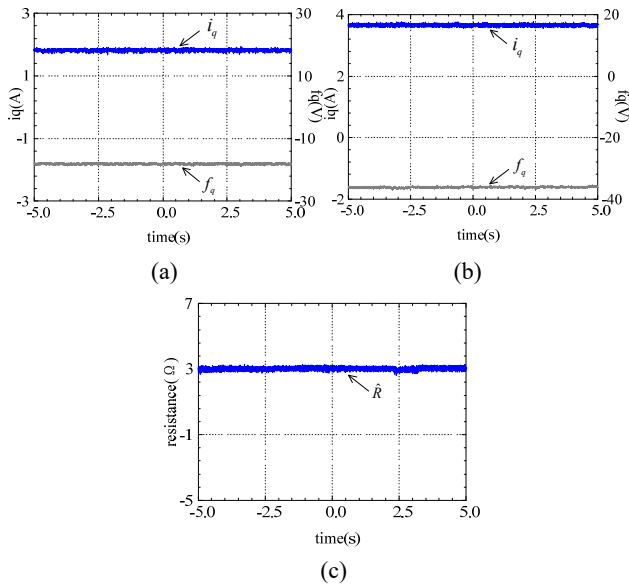


Fig. 7. Experimental results of the stator resistance estimation under  $R=4.3R_0$  at 1000r/min: (a) q-axis current and estimated  $\hat{i}_q$  with a 2N.m load; (b) q-axis current and estimated  $\hat{i}_q$  with a 4N.m load; (c) estimated stator resistance.

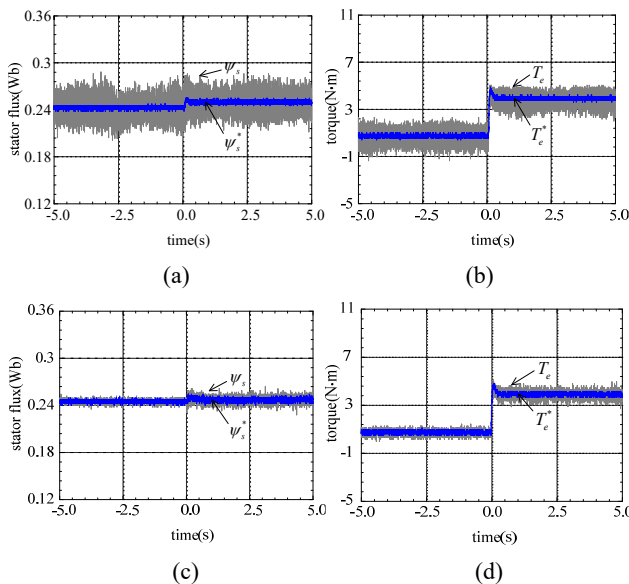


Fig. 8. Experimental results of both methods under  $L=1.5L_0$  at 500r/min: (a) stator flux reference and its response using the DB-DTC method; (b) torque reference and its response using the DB-DTC method; (c) stator flux reference and its response using the proposed method; (d) torque reference and its response using the proposed method.

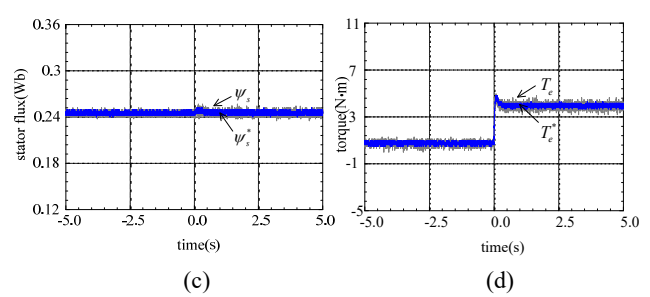
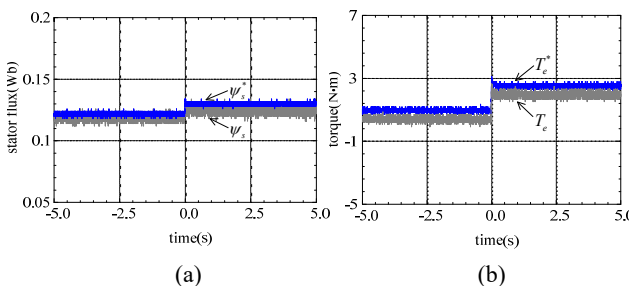


Fig. 9. Experimental results of both methods under  $\psi_f=0.5\psi_{f0}$  at 500r/min: (a) stator flux reference and its response using the DB-DTC method; (b) torque reference and its response using the DB-DTC method; (c) stator flux reference and its response using the proposed method; (d) torque reference and its response the using proposed method.

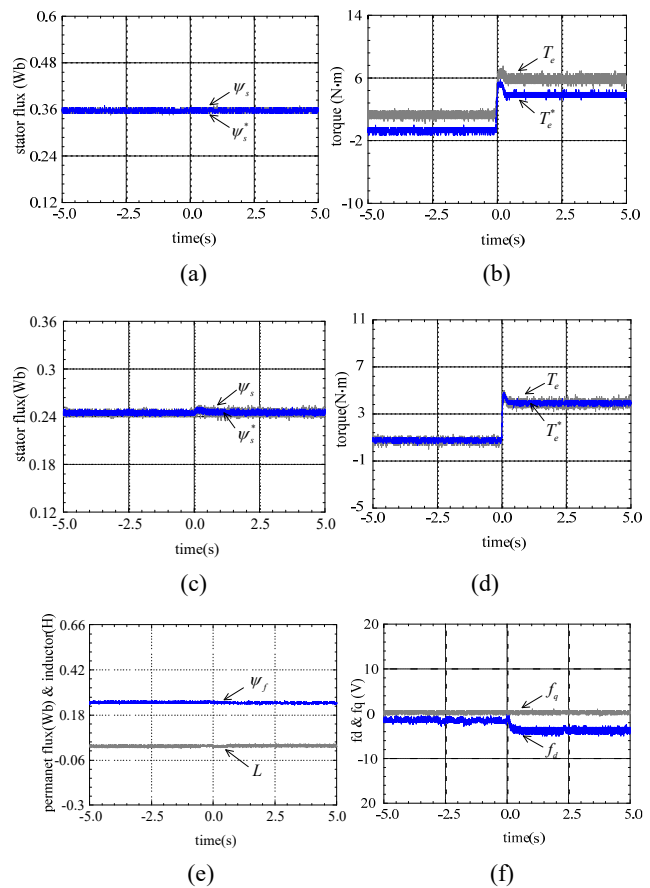


Fig. 10. Experimental results of both methods under  $L=0.66L_0$  and  $\psi_f=1.5\psi_{f0}$ : (a) stator flux reference and its response using the DB-DTC method; (b) torque reference and its response using the DB-DTC method; (c) stator flux reference and its response using the proposed method; (d) torque reference and its response using the proposed method; (e) estimation values of the stator inductance and permanent-magnetic flux linkage using the proposed method; (f) dq-axis disturbance estimation using the proposed method.

estimated, and that the tracking errors of the stator flux and torque caused by parameters changes can be effectively eliminated by using the proposed method.

## VII. CONCLUSIONS

An improved deadbeat direct torque control method is proposed and has been experimentally applied to a SPMSM drive system. The major contributions of this work include: 1) using an observer to achieve simultaneous parameter estimation and one-step delay compensation; 2) proposing a low parameter sensitivity deadbeat direct torque control method to improve the tracking performance of SPMSM derive systems in the presence of parameter mismatch.

## ACKNOWLEDGMENT

This work was sponsored in part by the research funds for the National Natural Science Foundation of China under Grants #51507004, by Beijing Natural Science Foundation under Grants #3172011, by Young Scholars Scientific Research Innovation Fund of North China University of Technology, and the Outstanding Young Scholars Fund of North China University of Technology under Grants XN018027.

## REFERENCES

- [1] G. S. Buja and M. P. Kazmierkowski, "Direct torque control of PWM inverter-fed AC motors – A survey," *IEEE Trans. Ind. Electron.*, Vol. 51, No. 4, pp. 744-757, Aug. 2004.
- [2] Y. Zhang and H. Yang, "Two-vector-based model predictive torque control without weighting factors for induction motor drives," *IEEE Trans. Power Electron.*, Vol. 31, No. 2, pp. 1381-1390, Sep. 2016.
- [3] W. Xie, X. Wang, F. Wang, W. Xu, R. M. Kennel, and R. D. Lorenz, "Finite-control-set model predictive torque control with a deadbeat solution for PMSM drives," *IEEE Trans. Ind. Electron.*, Vol. 62, No. 9, pp. 5402-5410, Sep. 2015.
- [4] J. S. Lee, C. Choi, J. Seok, and R. D. Lorenz, "Deadbeat-direct torque and flux control of interior permanent magnet synchronous machines with discrete time stator current and stator flux linkage observer," *IEEE Trans. Ind. Appl.*, Vol. 47, No. 4, pp. 1749-1758, Jul./Aug. 2011.
- [5] C. Choi, J. Seok, and R. D. Lorenz, "Wide-speed direct torque and flux control for interior PM synchronous motors operating at voltage and current limits," *IEEE Trans. Ind. Appl.*, Vol. 49, No. 1, pp. 109-117, Jan./Feb. 2013.
- [6] J. S. Lee, R. D. Lorenz, and M. A. Valenzuela, "Time optimal and loss minimizing deadbeat-direct torque and flux control for interior permanent magnet synchronous machines," *IEEE Trans. Ind. Appl.*, Vol. 50, No. 3, pp. 1880-1890, May/June 2014.
- [7] N. T. West and R. D. Lorenz, "Digital implementation of stator and rotor flux-linkage observers and a stator-current observer for deadbeat direct torque control of induction machines," *IEEE Trans. Ind. Appl.*, Vol. 45, No. 2, pp. 729-736, Mar./Apr. 2009.
- [8] K.-B. Lee and F. Blaabjerg, "Sensorless DTC-SVM for induction motor driven by a matrix converter using a parameter estimation strategy," *IEEE Trans. Ind. Electron.*, Vol. 55, No. 2, pp. 512-521, Feb. 2008.
- [9] Y. Wang, T. Ito, and R. D. Lorenz, "Loss manipulation capabilities of deadbeat direct torque and flux control induction machine drives," *IEEE Trans. Ind. Appl.*, Vol. 51, No. 6, pp. 4554-4566, Nov./Dec. 2015.
- [10] M. Saur, F. Ramos, A. Perez, D. Gerling, and R. D. Lorenz, "Implementation of deadbeat-direct torque and flux control for synchronous reluctance machines to minimize loss each switching period," *2016 IEEE Applied Power Electronics Conference and Exposition (APEC)*, pp. 215-220, 2016.
- [11] K. Wang, B. Chen, G. Shen, W. Yao, K. Lee, and Z. Lu, "Online updating of rotor time constant based on combined voltage and current mode flux observer for speed-sensorless AC drives," *IEEE Trans. Ind. Electron.*, Vol. 61, No. 9, pp. 4583-4593, Sep. 2014.
- [12] A. Yoo and S. Sul, "Design of flux observer robust to interior permanent-magnet synchronous motor flux variation," *IEEE Trans. Ind. Appl.*, Vol. 45, No. 5, pp. 314-322, Sep./Oct. 2009.
- [13] Z. Xu and M. F. Rahman, "An adaptive sliding stator flux observer for a direct-torque-controlled IPM synchronous motor drive," *IEEE Trans. Ind. Appl.*, Vol. 54, No. 5, pp. 2398-2406, Sep./Oct. 2007.
- [14] I. Boldea, M. Paicu, G. Andreescu, and F. Blaabjerg, "Active flux DTFCSVM sensorless control of IPMSM," *IEEE Trans. Energy Convers.*, Vol. 24, No. 2, pp. 314-322, Jun. 2009.
- [15] W. Xu and R. D. Lorenz, "Reduced parameter sensitivity stator flux linkage observer in deadbeat-direct torque and flux control for IPMSMs," *IEEE Trans. Ind. Appl.*, Vol. 50, No. 4, pp. 2636-2636, Jul./Aug. 2014.
- [16] X. Zhang, B. Hou, and Y. Mei, "Deadbeat Predictive Current Control of Permanent-Magnet Synchronous Motors with Stator Current and Disturbance Observer," *IEEE Trans. Power Electron.*, Vol. 32, No. 5, pp. 3818-3834, May, 2017.
- [17] G. Feng, C. Lai, K. Mukherjee, and N. C. Kar, "Current injection-based online parameter and VSI nonlinearity estimation for PMSM drives using current and voltage DC components," *IEEE Trans. Transport. Electrification.*, Vol. 2, No. 2, pp. 119-128, Feb. 2016.
- [18] Guodong Feng, Chunyan Lai and Narayan C. Kar "A novel current injection-based online parameter estimation method for PMSMs considering magnetic saturation," *IEEE Trans. Magn.*, Vol. 52, No. 7, 2016.
- [19] K. Liu, Z. Q. Zhu, Q. Zhang, and J. Zhang, "Influence of nonideal voltage measurement on parameter estimation in permanent-magnet synchronous machines," *IEEE Trans. Ind. Electron.*, Vol. 59, No. 6, pp. 2438-2447, Jun. 2012.
- [20] M. Rashed, P. F. MacConnell, and A. Fraser Stronach, "Nonlinear adaptive state-feedback speed control of a voltage fed induction motor with varying parameters," *IEEE Trans. Ind. Appl.*, Vol. 42, No. 3, pp. 723-732, May/June 2006.
- [21] Y. R. Kim, S. K. Sul, and M. H. Park, "Speed sensorless vector control of induction motor using extended kalman filter," *IEEE Trans. Ind. Appl.*, Vol. 30, No. 5, pp. 1225-1233, Oct. 1994.
- [22] Z. Q. Zhu, X. Zhu, and P. D. Sun, "Estimation of winding resistance and PM flux-linkage in brushless AC machines by reduced-order extended Kalman filter," in *Proc. IEEE Int. Conf. Netw., Sens. Control*, pp. 740-745, 2007.
- [23] Y. Wang, N. Niimura, and R. D. Lorenz, "Real-time

parameter identification and integration on deadbeat-direct torque and flux control (DB-DTFC) without inducing additional torque ripple,” *IEEE Trans. Ind. Appl.*, Vol. 52, No. 4, pp. 3104-3114, Jul./Aug. 2016.

- [24] H. Le-Huy, K. Slimani, and P. Viarouge, “Analysis and implementation of a real-time predictive current controller for permanent-magnet synchronous servo drives,” *IEEE Trans. Ind. Electron.*, Vol. 41, No. 1, pp. 110-117, Feb. 1994.
- [25] W. Xu and R. D. Lorenz, “High-frequency injection-based stator flux linkage and torque estimation for DB-DTFC implementation on IPMSMs considering cross-saturation effects,” *IEEE Trans. Ind. Appl.*, Vol. 50, No. 6, pp. 3805-3815, Nov./Dec. 2014.



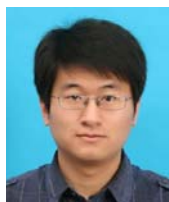
**Xiao-Guang Zhang** received his B.S. degree in Electrical Engineering from the Heilongjiang Institute of Technology, Harbin, China, in 2007; and his M.S. and Ph.D. degrees in Electrical Engineering from the Harbin Institute of Technology (HIT), Harbin, China, in 2009 and 2014, respectively. He is presently working as an Assistant Professor

at the North China University of Technology, Beijing, China. From 2012 to 2013, he was a Research Associate at the Wisconsin Electric Machines and Power Electronics Consortium (WEMPEC), University of Wisconsin–Madison, Madison, WI, USA. His current research interests include power electronics and electric machines drives.



**Ke-Qin Wang** was born in Henan, China, in 1991. He received his B.S. degree in Electrical Engineering from the Henan Institute of Science and Technology, Henan, China, in 2015. He is presently working towards his M.S. degree at the North China University of Technology, Beijing, China. His current research interests include

permanent magnet synchronous motor drives.



**Ben-Shuai Hou** was born in Shandong, China, in 1989. He received his B.S. degree in Electrical Engineering from the Beijing Union University, Beijing, China, in 2013. He is presently working towards his M.S. degree at the North China University of Technology, Beijing, China. His current research interests include PM machine

drives.